Shell-instability generated waves by low energy electrons on converging magnetic field lines

D. Sundkvist,[1,2] A. Vaivads,[2] Y. V. Bogdanova,[3] V. V. Krasnoselskikh,[1]
A. Fazakerley,[3] and P. M. E. Décréau[1]

Received 12 August 2005; revised 21 November 2005; accepted 16 December 2005; published 7 February 2006.

[1] Wave emissions at electron cyclotron harmonics and at frequencies above the local plasma frequency are commonly observed in different magnetospheric regions. We show that such emissions when observed in the cusp, mantle or polar cap can be generated by shell-type electron distributions. We present an example of observations of such shell type distributions having positive slope in velocity space at low energies, about 10 eV. Numerical calculations of wave growth rate based on the observed particle distributions show that the shell-instability can generate electrostatic and electromagnetic wave modes: whistler waves, electron cyclotron harmonics, upper-hybrid as well as the RX mode. Local wave spectra observations are consistent with the presence of all those wave modes in data. A possible connection between low and high frequency waves is discussed. Our results clearly show the importance of detailed studies of the lowest energy electrons.
Citation: Sundkvist, D., A. Vaivads, Y. V. Bogdanova, V. V. Krasnoselskikh, A. Fazakerley, and P. M. E. Décréau (2006), Shell-instability generated waves by low energy electrons on converging magnetic field lines, *Geophys. Res. Lett.*, *33*, L03103, doi:10.1029/2005GL024388.

1. Introduction

[2] Shell-like particle distributions are commonly observed in different space plasma environments such as the auroral zone, cusp, quasi-perpendicular shocks, comet pick-up ions, etc. Also common are partially developed shell distributions or shell distributions with a loss-cone that are referred to as horseshoe distributions. Ring distributions are also closely related to shell-like distributions. A common feature of all those distributions is that they are usually unstable and can generate different plasma waves, partially due to a positive slope $\partial f/\partial v_\perp$ in velocity space.

[3] Shell-type distributions of ions are known to be unstable to several ion wave modes (e.g., magnetosonic ion waves [*Perraut et al.*, 1982], lower-hybrid waves [*Bingham et al.*, 1999], ion-Bernstein and ion-cyclotron waves [*Janhunen et al.*, 2003; *Sundkvist et al.*, 2005]). As for electrons, the shell-instability is known since long to be a strong source for electron cyclotron waves [*Tataronis and Crawford*, 1970a, 1970b]. Recently the shell-maser has been put forward [*Pritchett et al.*, 1999; *Ergun et al.*, 2000; *Bingham and Cairns*, 2000] as a stronger source of free energy for auroral kilometric radiation (AKR) than the traditional loss-cone maser [*Wu and Lee*, 1979].

[4] In this paper we show that electron cyclotron harmonics and waves with frequencies above the local plasma frequency that are commonly observed on cusp, mantle and plasma lobe field lines can be due to shell-like distributions of electrons. In earlier studies it has been speculated that such emissions can be due to electron beams [*Menietti et al.*, 2002]. We present one event study based on Cluster electron and wave observations. We solve numerically the dispersion relation for modes of interest using realistic models of actually observed electron distributions. The obtained results have important implications for other regions where electron shell distributions have been observed or are present but due to the low energies involved have not been experimentally identified yet.

2. Observations

[5] We present data from a southern hemisphere inbound passage of the cusp/mantle/polar cap by the Cluster spacecraft during southward interplanetary magnetic field (IMF) conditions on the 3rd of March, 2002. In Figure 1a we show the electric field of natural emissions observed by the WHISPER instrument [*Décréau et al.*, 1997]. The plasma density was rather high and variable ($n \sim 10-30$ cm^{-3}) as indicated by the plasma frequency, $f_{pe} \sim 30-50$ kHz. The ambient magnetic field was $B_0 \sim 105$ nT, which gives the electron gyrofrequency $f_{ce} \sim 2.9$ kHz, Thus at all times in the analyzed interval the plasma is overdense, $f_{pe} \gg f_{ce}$.

[6] The most obvious wave modes present are intensive electron cyclotron harmonic (ECH) waves with up to 8 or 9 harmonics. These waves are most pronounced on quiet magnetic field lines (not shown) on the tailward side of the cusp, corresponding to mantle type plasma in the events we have analyzed. In addition continuous emissions are present for frequencies $f \gtrsim f_{pe}$. Also present are whistler-type waves in the lower-hybrid range ($\sim$70 Hz) detected by other instrument (WBD), not shown here.

[7] We observe almost no ECH waves simultaneously with strong field aligned electron beams, as has been previously reported [*Menietti et al.*, 2002]. In our case ECH waves are generally observed when the distribution function deviates from a Maxwellian at low energies. At those energies the phase space density is lower than that for a Maxwellian and the distributions are of a flat-top type. Figure 2 shows a typical electron distribution function observed at 22:23:25 UT by the PEACE instrument [*Johnstone et al.*, 1997]. The flat-top distributions have

[1]Laboratoire de Physique et Chimie de l'Environnement, CNRS, Orléans, France.
[2]Swedish Institute of Space Physics, Uppsala, Sweden.
[3]Mullard Space Science Laboratory, University College London, Holmbury St. Mary, Dorking, UK.

0094-8276/06/2005GL024388

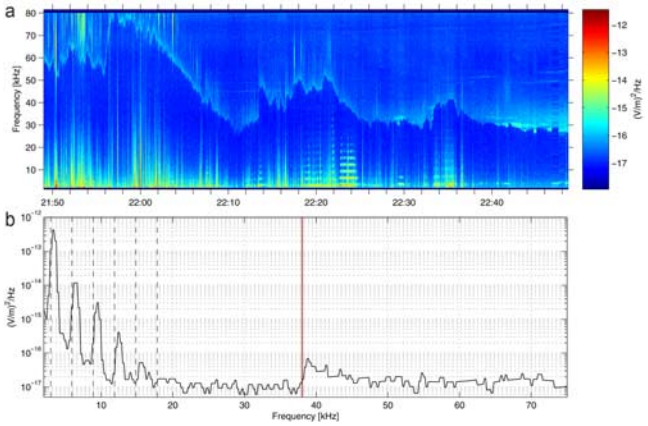

Figure 1. (a) Frequency versus time spectrogram when Cluster spacecraft 1 passed inbound through cusp/mantle on the southern hemisphere on 3rd of March 2002. (b) Power spectral density of electric field at 22:23:25 UT. The electron cyclotron harmonics and continuous emissions above $f_{pe} \sim f_{UH}$ are clearly visible. Dotted vertical lines are multiples of f_{ce}, black solid vertical line shows f_{pe} and the red line the upper hybrid frequency f_{UH}.

generally a positive slope $\partial f/\partial v$ in the energy range 8–20 eV. This slope is present in all directions but usually strongest in the perpendicular one. During the time of measurement the spacecraft was positively charged to +3.3 V, as derived from the probe to spacecraft potential measured by the EFW instrument [*Gustafsson et al.*, 1997]. We have corrected the observed distribution functions for this value, and carefully checked that photoelectrons do not contaminate the measurements at the energies were the slopes are observed. To investigate if the positive slopes in the electron distribution can be a source of free energy for the observed waves we model the observed distributions

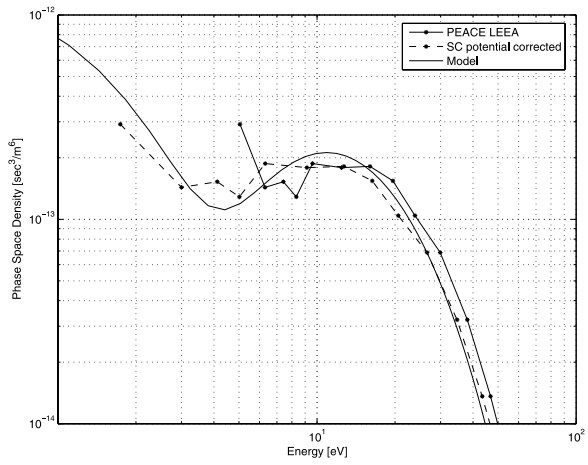

Figure 2. Low energy part of the electron distribution function on Cluster spacecraft 1 at 2002-03-03 22:23:25 UT. Solid line with dots shows measured electrons distribution from PEACE LEEA sensor at 90° pitch angle. It shows a typical $\partial f/\partial v_{\perp}$ slope when waves are present. Dashed line shows the spacecraft potential corrected distribution function. Thin solid line shows a model distribution function used for instability calculations.

Table 1. Parameters Used for Maxwellian Model of Observed Particle Data[a]

	q [$\|e\|$]	n^j [cm^{-3}]	T^j [eV]
e_1^-	−1	45	9
e_2^-	−1	−28	4.4
e_3^-	−1	5	1.5
e_4^-	−1	2	2
p_1	+1	24	100

[a]The plasma model is defined as $f(v) = \Sigma_j\, n^j(\sqrt{\pi}v_{th}^j)^{-3}\exp\,[-(v/v_{th}^j)^2]$.

(Figure 2) and calculate the wave growth obtained from the model.

3. Numerical Dispersion Relations

[8] To study wave instability based on actual plasma conditions, we used the numerical dispersion relation solver WHAMP [*Rönnmark*, 1982]. To model the observed particle distributions a sum of four Maxwellians for the electrons and one for the protons were used, see Table 1. The modeled electron distribution function is shown together with the observed one in Figure 2.

[9] Some of the obtained linear modes present in this plasma are shown in Figure 3 as a perspective plot of the dispersion surfaces [*André*, 1985]. This representation gives good simultaneous information of frequency as well as wave vectors k. Displayed are parts of the dispersion surfaces for the whistler mode and some of the first electron cyclotron harmonic modes [*Lominadze*, 1981]. Not all modes present in the plasma are shown. In Figure 3 the first cyclotron mode around f_{ce} is electromagnetic for perpendicular propagation, while the modes at 1.1–1.9 f_{ce} and 2.1–2.9 f_{ce} are electrostatic. The surfaces are colored after the logarithm of γ/ω_{ce}, where γ is the growth rate and $\omega_{ce} = 2\pi\, f_{ce}$. Blue/red corresponds to negative/positive values, i.e., damping/growth respectively. We note that growth occurs on all these modes, but for different k-vectors. Substantial growth occurs also on the upper-hybrid surface (Figure 4). If the surfaces are cut ending in dark blue color, this means that the damping rate is too strong for the mode to exist. This is

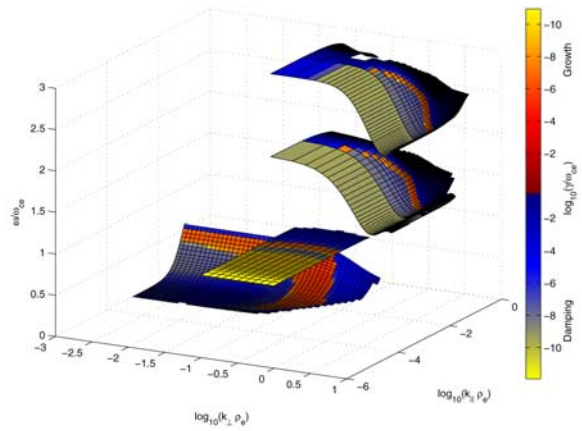

Figure 3. Dispersion surfaces for the plasma model in Table 1. Shown are in order from lower to higher frequency: whistler surface and three electron cyclotron (EC) modes (f_{ce}, 1.1–1.9f_{ce}, 2.1–2.9 f_{ce}). The scale is color coded after $log_{10}(\gamma/\omega_{ce})$. The color scale is chosen to display damping (blue) and growth (red).

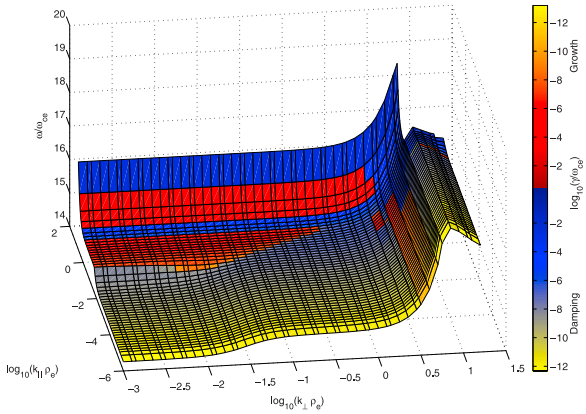

Figure 4. Dispersion surface of upper-hybrid waves. For perpendicular propagation this is sometimes called the slow electrostatic extraordinary mode, and for small $k_\perp$ it corresponds to the electromagnetic Z-mode. In regions of growth it is electrostatic. Color representation as in Figure 3.

for example the case for the resonance cone of the whistler surface for large values of $k_\perp$. It should be noted that for the sake of visibility not all moderately damped parts of the surfaces are displayed.

[10] In Figure 5 we display the dispersion surface of the RX mode when $f > f_R$, the R mode cut-off frequency, which is comparable to f_{pe} and f_{UH}. We note that for oblique propagation angles and short perpendicular wavelengths, $k_\perp \rho_e \geq 0.1$ there exists considerable growth. The waves just outside this region are heavily damped. The LO mode (not shown) display insignificant growth and are only moderately damped. Thus we expect the waves above f_{pe} to be right hand polarized. This cannot be tested with the existing data set.

[11] For all displayed modes the maximum temporal growth rate is of the order $\gamma/\omega_{ce} \sim 10^{-4} - 10^{-5}$. We have tested that the growth rate scales with the positive slope such that increasing the slope by a factor of two increases the maximum growth rate by a factor of two. The obtained growth rates correspond to a characteristic growth time of about 1–10 s. While this growth rate is clearly too small to explain the observed spectral changes at scales much shorter than 1 s, it is worth noting some important points. 1) For large $k_\perp$ values the wave group velocity can be low enough that even for slow temporal growth rates the waves stay long enough time inside the generation region and thus can obtain significant amplitudes. In other words the spatial growth rate $-\gamma/|\partial\omega/\partial k_\perp|$ may become significant even though the temporal growth rate is small. 2) The energy resolution of the particle instrument does not allow us to resolve the steepest gradients in the distribution functions and thus most probably they are underestimated. 3) The observed distribution functions are averages over ~0.1 s, a time scale much longer than the wave period. If we observe quasi-stationary wave activity we will almost always observe a slope in velocity space when the instability is already saturated and thus our model will underestimate the growth rate, possibly with several orders of magnitude.

4. Discussion and Conclusions

[12] In this paper we have shown that a large part of the wave emissions that are observed in the cusp/mantle plasma are most probably generated by shell-like electron distribution functions. These distributions have positive derivatives in velocity space at low energies, typically less than a few tens of eV. This makes it difficult to observe them and probably is one of the reasons why this free energy source has not been suggested before. In the case that we discuss the plasma is overdense ($f_{pe} \gg f_{ce}$). Numerical calculations of growth rate from a plasma model based on observed electron distribution functions predict wave growth at the whistler, multiple electron cyclotron, upper-hybrid and the RX modes. Observations of waves show striking agreement with the predicted frequency range.

[13] An important question is what are the possible mechanisms of the shell formation. Shell-like distributions functions can form due to time-of-flight effects on runaway electron distributions from a distant source. The time-of-flight effect would lead to the creation of electron beams while owing to the conservation of the first adiabatic invariant in the converging magnetic field these electrons would spread to larger pitch angles and form shell-type distributions. These time of flight effects are most probably unimportant in our case; electrons move much faster than ions, but during our interval for a period of minutes we observe electrons together with ions of what we believe is of the same origin (magnetosheath). Thus we would expect to see time of flight effects in ions while electrons all the time adjust to keep quasineutrality.

[14] Instead we can argue that the shells can be due to acceleration of electrons by low frequency waves such as dispersive Alfvén waves or ion cyclotron waves that are ubiquitous on these field lines [e.g., *Chaston et al.*, 2003; *Sundkvist et al.*, 2005]. We can make a rough estimate of the parallel potential the electrons would experience within such waves. We observe electric fields with a peak-to-peak amplitude of $E_{pp\perp} = 0.5 - 1$ mV/m at frequencies around the proton gyrofrequency. Earlier work [*Sundkvist et al.*, 2005] and also a rough estimate from comparisons between two satellites that are on closest field lines (C2 and C3)

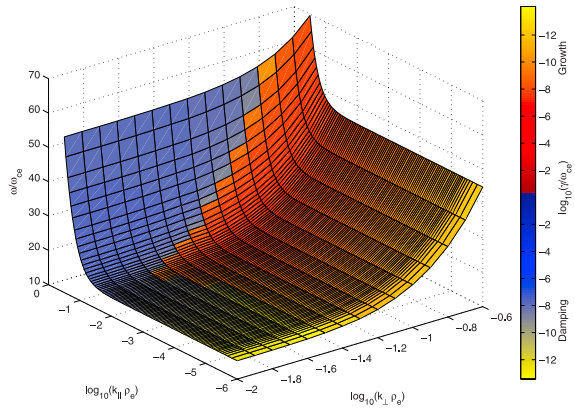

Figure 5. Dispersion surface of the RX mode (color as in Figures 3 and 4). For parallel propagation this mode corresponds to the right-handed electromagnetic R-mode, which is heavily damped for this electron distribution function. For perpendicular propagation it corresponds to the X-mode, which here show insignificant damping and growth respectively. The strongest growth is found for oblique propagation for rather short perpendicular wavelengths.

show that for these waves $\lambda_\perp \leq 2 - 4\rho_i$. For such wavelengths both kinetic Alfvén waves and ion cyclotron waves are of mainly electrostatic character and therefore the parallel potential within these waves is comparable to the perpendicular potential which can be estimated. For the present plasma parameters $\rho_s \simeq \rho_i \simeq 30$ km which gives the potential $\phi_\parallel \sim \phi_\perp \sim (E_{pp\perp}/2)(\lambda_\perp/2)/\sqrt{2} \sim 5-20$ V and is in agreement with the energy of the positive slopes in the electron distribution functions. This indicates that indeed there could be a relation between low and high-frequency wave phenomena in the cusp plasma. The field aligned electric field sustained by the waves around the proton cyclotron frequency accelerates electrons in parallel direction, which pitch angle spread in the converging magnetic field and form shell-type distributions. These unstable distributions subsequently generate whistler, electron cyclotron harmonics, upper-hybrid and RX waves as shown. While we have only presented rough estimates the future work should analyze in details the coupling between low and high frequency waves. In addition, this letter has been limited to the regime of linear growth. The nonlinear interaction and saturation of these wave modes is a topic for our future study and will be published elsewhere.

[15] While in this paper we have analyzed the cusp/mantle region the results can be important also for other regions in space, e.g., boundary layers near the magnetopause or plasma sheet. We have analyzed the overdense case but it would be interesting to see whether similar generation mechanisms work also in the underdense case; the ability of a shell to produce electrostatic as well as electromagnetic modes simultaneously could have important implications. We postpone the analysis of other regions in space and the underdense case to a future study.

[16] **Acknowledgments.** This research was partially supported by the European Community under contract HPRN-CT-2001-00314. AV research is supported by the Swedish Research Council. We thank P. Décréau and the WHISPER team, A. Fazakerley and the PEACE team and A. Balogh and the FGM team for the data. We also thank M. André and M. Mooroka for useful discussions.

References

André, M. (1985), Dispersion surfaces, *J. Plasma Phys*, *33*, 1–19.

Bingham, R., and R. A. Cairns (2000), Generation of auroral kilometric radiation by electron horseshoe distributions, *Phys. Plasmas*, *7*, 3089–3092.

Bingham, R., B. J. Kellett, R. A. Cairns, R. O. Dendy, and P. K. Shukla (1999), Wave generation by ion horseshoe distributions on auroral field lines, *Geophys. Res. Lett.*, *26*, 2713–2716.

Chaston, C. C., J. W. Bonnell, C. W. Carlson, J. P. McFadden, R. E. Ergun, and R. J. Strangeway (2003), Properties of small-scale Alfvén waves and accelerated electrons from FAST, *J. Geophys. Res.*, *108*(A4), 8003, doi:10.1029/2002JA009420.

Décréau, P. M. E., et al. (1997), Whisper, a resonance sounder and wave analyser: Performances and perspectives for the Cluster mission, *Space Sci. Rev.*, *79*, 157–193.

Ergun, R. E., C. W. Carlson, J. P. McFadden, G. T. Delory, R. J. Strangeway, and P. L. Pritchett (2000), Electron-cyclotron maser driven by charged-particle acceleration from magnetic field-aligned electric fields, *Astrophys. J.*, *538*, 456–466.

Gustafsson, G., et al. (1997), The electric field and wave experiment for the Cluster mission, *Space Sci. Rev.*, *79*, 137–156.

Janhunen, P., A. Olsson, A. Vaivads, and W. K. Peterson (2003), Generation of Bernstein waves by ion shell distributions in the auroral region, *Ann. Geophys.*, *21*, 881–891.

Johnstone, A. D., et al. (1997), Peace: A Plasma Electron and Current Experiment, *Space Sci. Rev.*, *79*, 351–398.

Lominadze, D. G. (1981), *Cyclotron Waves in Plasma*, Elsevier, New York.

Menietti, J. D., O. Santolik, J. D. Scudder, J. S. Pickett, and D. A. Gurnett (2002), Electrostatic electron cyclotron waves generated by low-energy electron beams, *J. Geophys. Res.*, *107*(A10), 1285, doi:10.1029/2001JA009223.

Perraut, S., A. Roux, P. Robert, R. Gendrin, J.-A. Sauvaud, J.-M. Bosqued, G. Kremser, and A. Korth (1982), A systematic study of ULF waves above FH+ from GEOS 1 and 2 measurements and their relationships with proton ring distributions, *J. Geophys. Res.*, *87*, 6219–6236.

Pritchett, P. L., R. J. Strangeway, C. W. Carlson, R. E. Ergun, J. P. McFadden, and G. T. Delory (1999), Free energy sources and frequency bandwidth for the auroral kilometric radiation, *J. Geophys. Res.*, *104*, 10,317–10,326.

Rönnmark, K. (1982), Waves in homogeneous, anisotropic multicomponent plasmas (WHAMP), technical report, Kiruna Geophys. Inst., Kiruna, Sweden.

Sundkvist, D., et al. (2005), Multi-spacecraft determination of wave characteristics near the proton gyrofrequency in high-altitude cusp, *Ann. Geophys.*, *23*, 983–995.

Tataronis, J. A., and F. W. Crawford (1970a), Cyclotron harmonic wave propagation and instabilities I. Perpendicular propagation, *J. Plasma Phys.*, *4*, 231–248.

Tataronis, J. A., and F. W. Crawford (1970b), Cyclotron harmonic wave propagation and instabilities II. Oblique propagation, *J. Plasma Phys.*, *4*, 249–264.

Wu, C. S., and L. C. Lee (1979), A theory of the terrestrial kilometric radiation, *Astrophys. J.*, *230*, 621–626.

Y. V. Bogdanova and A. Fazakerley, Mullard Space Science Laboratory, University College London, Holmbury St. Mary, Dorking, Surrey RH5 6NT, UK.

P. M. E. Décréau, V. V. Krasnoselskikh, and D. Sundkvist, Laboratoire de Physique et Chimie de l'Environnement, CNRS, F-45071 Orléans, France. (davids@irfu.se)

A. Vaivads, Swedish Institute of Space Physics, SE-75121 Uppsala, Sweden.